Migration of Protons during the Excited-State Tautomerization of Aqueous 3-Hydroxyquinoline

Hyunung Yu,† Oh-Hoon Kwon, and Du-Jeon Jang*

School of Chemistry, Seoul National University, NS60, Seoul 151-742, Korea

Received: December 8, 2003; In Final Form: April 26, 2004

The detailed mechanism of proton transfer and the individual catalytic roles of H_2O, H_3O^+, and OH^- in the excited-state tautomerization of aqueous 3-hydroxyquinoline are determined by measuring fluorescence kinetic constants as functions of wavelength, pH, hydrogen isotope, and temperature. The molecule undergoes tautomerization in a stepwise manner by forming an anionic intermediate and the tautomer on time scales of 600 and 1200 ps, respectively, in the pH region of 7−8. However, the intermediate transforms rapidly into the tautomer in the pH region of 4−6 owing to the migration of the proton concurrently formed with the intermediate. This provides experimental evidence of the idea that the extremely fast migration of protons in water occurs by continuously forming and breaking hydrogen bonds involved in hydrated proton clusters.

Introduction

Proton transfer has been attracting considerable attention because it plays a key role in a wide variety of chemical and biological phenomena.[1−6] Recent interest is on the dissociation dynamics of a proton from an acid[7−10] and on the dispersion dynamics of hydrated proton clusters in bulk solvents.[11−14] The proton-transfer dynamics is determined by the size, the structure, and the motion of a solvent cluster involved as well as by the nature of a prototropic group,[7−10,15−17] whereas the rate of proton migration is controlled by solvent structural dynamics.[11−14]

Proton transfer by the catalysis of water is fundamentally important but enormously complicated. The dynamics and mechanism of excited-state proton transfer to water have been often investigated with photoacids.[18−21] The most important feature controlling the extremely fast excited-state proton transfer to an aqueous medium is the formation of a specifically structured water cluster.[4,7] Water clusters having 4 ± 1 molecules have been suggested to be the proton acceptors of photoacids.[20−24] Proton-transfer studies employing various 1- and 2-naphthol derivatives have indicated that the apparent sizes of the accepting water clusters also depend on the acidity of the proton donors. In the case where a photoacidic group and a photobasic group exist in a molecule, a photon may initiate the protonation of the basic group and the deprotonation of the acidic group to yield a zwitterionic tautomer in water. Studies on proton transfer for this type of molecule, having as many as four potential wells in the first excited singlet state only, are interesting because the processes may serve as experimental models for proton migration and proton pumps in biological molecular systems.

In this regard, hydroxyquinolines and their derivatives, having two prototropic groups of enol and imine, are extensively explored.[16,17,25−39] 7-Hydroxyquinoline is known to form an intramolecular hydrogen-bonding chain, through which proton relay can take place during excited-state tautomerization.[16,25−28]

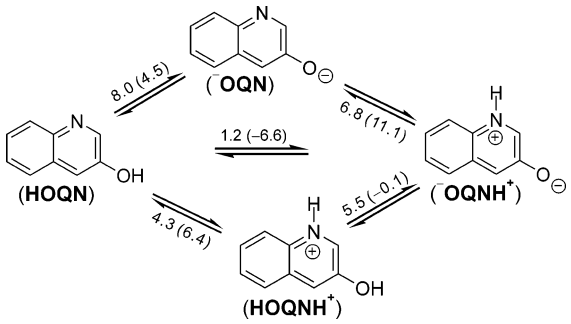

Figure 1. Ground-state equilibria among the prototropic species of 3HQ in water. The values of pK (pK*) and pK_a (pK_a*), except those for HOQN → $^-$OQNH$^+$, shown inside are taken from ref 38.

However, 6-hydroxyquinoline cannot form intramolecular hydrogen bonds because of its geometry.[34] Therefore, it undergoes tautomerization stepwise in water via forming prototropic intermediate species.[17,39] The individual catalytic roles of H_2O, H_3O^+, and OH^- as well as the involvement of solvent structural dynamics in the deprotonation of the enol group and in the migration of a hydrated proton cluster have been reported in the tautomerization reaction of 6-hydroxyquinoline.[17] As a comparative study, 3-hydroxyquinoline (3HQ), the photoacidic and photobasic groups of which are in close proximity to each other, is considered to be a good candidate for the evaluation of the solvent structural dynamics in the migration of protons in water. 3HQ in water exists as one of four prototropic species: the normal form (HOQN), the imine-protonated cation ($HOQNH^+$), the enol-deprotonated anion ($^-$OQN), and the zwitterionic tautomer ($^-OQNH^+$), as described in Figure 1. The $^-OQNH^+$ species undergoes electron rearrangement rapidly in the first excited singlet state to form the quinonoid tautomer (OQNH) in Figure 2 (vide infra). The ground-state equilibrium constants[38] of Figure 1 indicate that 3HQ in water exists almost exclusively in $HOQNH^+$, HOQN, and $^-$OQN at pH values of 2, 6, and 10, respectively, although 6% of 3HQ exists as $^-OQNH^+$ at pH 6. Thus, we can initiate the proton-transfer reactions of desired prototropic species by exciting aqueous 3HQ solutions with representatively selected pH values.

* To whom correspondence should be addressed. E-mail: djjang@plaza.snu.ac.kr. Phone: +82-2-875-6624. Fax: +82-2-889-1568.

† Present address: Department of Chemistry, University of Illinois at Urbana-Champaign, Urbana, Illinois 61801.

10.1021/jp031293w CCC: $27.50
Published on Web 06/18/2004

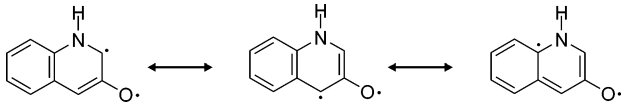

Figure 2. Resonance forms of OQNH produced via electron rearrangement immediately following the formation of $^{-}$OQNH^{+} in the first excited singlet state.

To our knowledge, we have measured, for the first time, the fluorescence kinetics and spectra of 3HQ prototropic species as functions of wavelength, pH, hydrogen isotope, and temperature to explore the excited-state tautomerization mechanism of aqueous 3HQ. In the present paper, we also report the pH-dependent catalytic roles of H_3O^+, OH^-, and H_2O in the tautomerization of 3HQ. Our results support the idea that the extremely fast migration of protons in water occurs by continuously forming and breaking hydrogen bonds involved in hydrated proton clusters.

Experimental Section

Materials. 3HQ was synthesized following ref 40 and purified twice via column chromatography. Aqueous solutions of 3^1HQ and 3^2HQ were prepared by dissolving 3HQ in triply distilled water and in ^2H_2O (isotopic purity $\geq$99.9%) purchased from Sigma, respectively. The p^{1}H and p^{2}H of 3HQ aqueous solutions were adjusted by adding ^{1}HCl/NaO^{1}H and ^{2}HCl/NaO^{2}H solutions, respectively. All the p^{2}H values were corrected from pH-meter measurements.[41] The concentration of 3HQ was 0.2 mM throughout the experiments. Sample temperatures were controlled using a refrigeratory bath circulator (Jeio Tech, RC-10V).

Measurements. Absorption spectra were measured by using a UV/vis spectrometer (Scinco, S-2040). Fluorescence spectra were obtained by using a homebuilt fluorimeter consisting of a 75-W Xe lamp (ARC, XS 432), a 0.30-m monochromator (ARC, Spectrapro 300), and a photomultiplier tube (ARC, PD 438). Fluorescence spectra were not corrected for the wavelength-dependent sensitivity variation of the detector.

An actively/passively mode-locked Nd:YAG laser (Quantel, YG701) and a 10-ps streak camera (Hamamatsu, C2830) attached to a CCD detector (Princeton Instruments, RTE128H) were employed for excitation and detection, respectively. Samples were excited by pulses of 25 ps and 315 nm generated through a Raman shifter, which was filled with methane at 15 atm and pumped by the fourth-harmonic pulses (266 nm) of the laser. Emission wavelengths (λ_{em}) were selected by combining band-pass filters. Fluorescence kinetic parameters were extracted by fitting measured kinetic profiles to computer-simulated curves, convoluted with instrumental response functions, of exponential rise followed by exponential decay. Unless specified otherwise, all measurements were carried out in ^1H_2O at 25 °C.

Results and Discussion

Absorption and Emission Spectra. The lowest-absorption bands of aqueous 3HQ prototropic equilibrium species are spectrally well distinguishable (Figure 3). The lowest absorption of HOQNH$^+$ at pH 2 gives the maximum at 340 nm. However, the emission spectrum obtained by exciting HOQNH$^+$ shows exclusively tautomeric fluorescence having the maximum at 450 nm without showing HOQNH$^+$ fluorescence expected to be located around 410 nm.[38] This implies that the deprotonation process of HOQNH$^+$ to form $^-$OQNH$^+$ is very facile (vide infra). The peak for the lowest-absorption band of $^-$OQN at pH 10 is located at 350 nm. The excitation of $^-$OQN gives rise to a fluorescence spectrum at 413 nm emitted mainly from $^-$OQN with a shoulder of tautomeric fluorescence at 450 nm, suggesting that the protonation of $^-$OQN is much slower than the deprotonation of HOQNH$^+$ (vide infra). The absorption spectrum at pH 6 shows a maximum at 320 nm arising from HOQN absorption and a shoulder around 370 nm originating from $^-$OQNH$^+$ absorption. The selective excitation of HOQN gives us an emission spectrum that is more complicated than that obtained from the excitation of $^-$OQN. A satellite band around 360 nm and the main band at 450 nm are unambiguously attributed to normal and tautomeric fluorescence, respectively. The difference spectrum constructed by multiplying the emission spectrum of pH 2 by 0.87 and subtracting the multiplied spectrum from the emission spectrum at pH 6 shows the maximum at 410 nm. The tautomerization of HOQN to $^-$OQNH$^+$ involves protonation to the imino group and deprotonation from the enol group. Then which process occurs first, or do the two processes take place simultaneously? The difference spectrum containing emission from the intermediate species of $^-$OQN around 410 nm hints that the tautomerization of HOQN to form $^-$OQNH$^+$ proceeds in a stepwise manner via the formation of $^-$OQN as the reaction intermediate (vide infra).

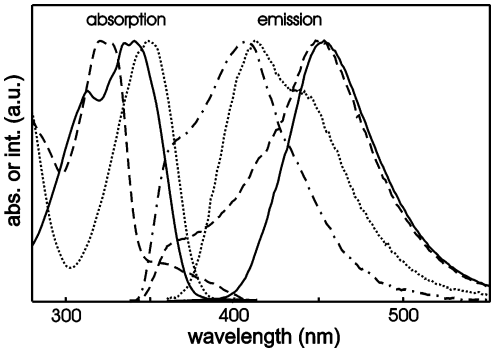

Figure 3. Absorption and emission spectra of aqueous 3HQ solutions at pH values of 2 (solid line), 10 (dotted line), and 6 (dashed line). Each sample was excited at the wavelength showing its absorption maximum. The dotted-dashed spectrum was constructed by multiplying the solid spectrum by 0.87 and subtracting the multiplied spectrum from the dashed spectrum.

Fluorescence Kinetics. Figure 4a at pH 2 shows that HOQNH$^+$ fluorescence at 400 nm decays on the time scale of 60 ps, whereas tautomeric fluorescence gives a concomitant rise time of 60 ps and a decay time of 5300 ps (Table 1). This indicates that the proton transfer of HOQNH$^+$ to a water cluster occurs within 60 ps to form $^-$OQNH$^+$ (pK_a* $= -0.1$).[38] The extreme lifetime difference now explains why HOQNH$^+$ fluorescence at pH 2 is negligibly weak compared to tautomeric fluorescence in Figure 3. However, Figure 4b at pH 10 indicates that $^-$OQN fluorescence decays on the time scale of 1200 ps and that tautomeric fluorescence rises on the same time scale of 1200 ps and decays in 5300 ps. Thus, the protonation of $^-$OQN from a water cluster takes place in 1200 ps to form $^-$OQNH$^+$ (pK_a* $= 11.1$).[38] Note that the protonation of $^-$OQN to form $^-$OQNH$^+$ is much slower than the deprotonation of HOQNH$^+$. This is often explained by the phenomena of intramolecular electronic charge transfer in excited and ground states.[7,18,19] The intermolecular proton-transfer rates of photoacids and photobases are closely related to the excess stabilization energies of their respective conjugates that render proton transfer highly exothermic and facile. The energy of HOQNH$^+$ (having the lowest absorption at 29 410 cm^{-1}), which is larger than that of $^-$OQN (having the absorption at 28 570 cm^{-1}),

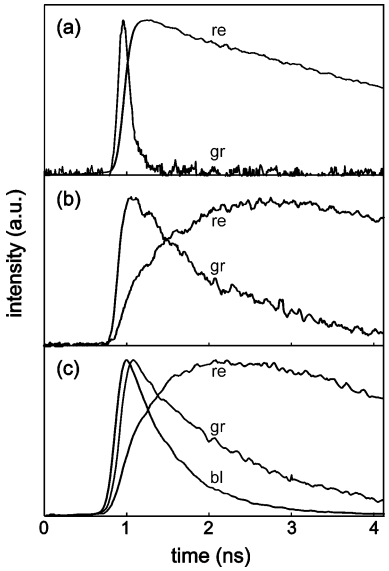

Figure 4. Fluorescence kinetic profiles of aqueous 3HQ solutions at pH values of 2 (a), 10 (b), and 6 (c). Samples were excited at 315 nm, and emission was collected at 350 ± 20 (bl), 400 ± 5 (gr), and 500 ± 5 nm (re).

TABLE 1: Fluorescence Kinetic Constants of Aqueous 3HQ at 25 °C

λ_{em} (nm)	pH	rise time (ps)	decay time (ps)	monitored species
400 ± 5	2	instant	60	$HOQNH^+$
500 ± 5	2	60	5300	OQNH
400 ± 5	10	instant	1200	^-OQN
500 ± 5	10	1200	5300	OQNH
350 ± 20	6	instant	600	HOQN
400 ± 5[a]	6	600	1200	^-OQN
500 ± 5	6	730	5300	OQNH

[a] The kinetics of pH 6 at 400 nm was fit to the function $I(t) = 0.18\exp(-t/60\text{ ps}) + 0.38\exp(-t/600\text{ ps}) + 0.44\{1 - \exp(-t/600\text{ ps})\}\exp(-t/1200\text{ ps})$. The first term is from the fluorescence interference of $HOQNH^+$ formed by the reaction of HOQN with hydrated proton clusters or directly excited from the ground state, whereas the second term is from the red-tailed interference of HOQN fluorescence. The fractional amplitude of the second term becomes large because we chose λ_{em} shifted to the blue by 10 nm from the maximum fluorescence wavelength of ^-OQN to avoid the interference of OQNH fluorescence. However, the fractional amplitude of the third term is not dominant because the intermediate generated via eq 1 is depleted rapidly by migrated protons without showing the intermediate fluorescence of ^-OQN (vide infra).

explains why the generation of $^-OQNH^+$ from $HOQNH^+$ is kinetically more feasible than that from ^-OQN.

The excitation of HOQN at pH 6 gives three distinctive fluorescence kinetic profiles of HOQN at 350 nm, intermediate species at 400 nm, and tautomeric species at 500 nm (Figure 4c). The kinetics at 350 nm indicates that the enol deprotonation of HOQN takes place on the time scale of 600 ps,which is 10 times longer than the enol-deprotonation time (60 ps) of $HOQNH^+$ (Table 1). The same decay kinetics of intermediate emission as that of ^-OQN emission clarifies that, as suggested by the fluorescence spectra of Figure 3, HOQN in water undergoes excited-state tautomerization stepwise via forming ^-OQN as the intermediate species. Although this is complicated because of interference luminescence (refer to the footnote of Table 1), it reveals that intermediate emission rises on the same time scale of 600 ps as the decay time of HOQN and decays on the same time scale of 1200 ps as the decay time of ^-OQN. The formation of ^-OQN, rather than $HOQNH^+$, as the selective reaction intermediate of the tautomerization can also be rationalized with principles involved in intramolecular electronic charge transfer. Because the lowest absorption energy of ^-OQN is smaller than that of $HOQNH^+$, the deprotonation of the enol group in the precursor of HOQN is expected to be more exothermic and more facile than the protonation of the imino group (vide supra). The fact that protonation to nitrogen is much slower than deprotonation from oxygen in both normal and intermediate species as well as in other aqueous hydroxyquinolines is certainly notable.[17,32,42] This implies that the photoacidity of the enol group is much stronger than the photobasicity of the imino group in excited hydroxyquinolines.

It is quite intriguing that the observed formation time (730 ps) of tautomeric emission is shorter than the observed decay time (1200 ps) of ^-OQN emission (Figure 4c and Table 1). This discrepancy indicates that there is another fast channel for the tautomerization. It will be shown in the final section that the fast pathway is the immediate depletion of ^-OQN intermediate anions by rapidly migrating protons released during the deprotonation of aqueous 3HQ. The direct proton relay of HOQN via a hydrogen-bond bridge formed with solvent molecules, as found in the case of 7-hydroxyquinoline in alcoholic solvents,[16,25] was discarded because tautomeric fluorescence was not observable at all in methanol solutions. Fast proton transfer via a bent H-bond wire around the aromatic ring is also excluded because at least three water molecules are required to form the wire. The extensive H-bonding nature of water results in large solvent aggregation and prevents the formation of a cyclically H-bonded structure; it has been found that only a 6.6×10^{-4} fraction of 7-azaindole molecules form cyclically H-bonded 1:1 complexes with solvent molecules in water.[43,44] Direct proton transfer within dimers[37] is also ruled out because dimeric association is not reported for any hydroxyquinolines in water. We consider the fact that dimer formation is not plausible, especially for 3HQ because of its unfavorable geometry for H bonding.

The kinetic isotope effects (KIEs) of enol deprotonation for $HOQNH^+$ and HOQN are 3.0 and 2.2, respectively, whereas the KIE of imine protonation for ^-OQN is 1.8 (Table 1). These KIE values are larger than the KIE (1.4) of proton migration in water originating from the cleavage of hydrogen bonds.[45] Both the deprotonation of the enol group and the protonation of the imino group are slower than either the formation or the dissociation of water clusters.[12] Thus, considering the rates and the KIEs, we suggest that the proton transfer of 3HQ prototropic species is an activated processes with tunnel effects (vide infra).

Solvatochromism of Tautomer Fluorescence. The reverse proton transfer of $^-OQNH^+$ to form either ^-OQN or $HOQNH^+$ does not occur in our studied range of pH, although a hydroxide ion having a large diffusion rate constant of $3 \times 10^{10}\ M^{-1}\ s^{-1}$ or a hydronium ion having a large diffusion rate constant of $7 \times 10^{10}\ M^{-1}\ s^{-1}$ can diffuse to the tautomer to form ^-OQN or $HOQNH^+$, respectively,[21,42] within the long lifetime (5300 ps) of tautomeric emission. We attribute the lack of reverse reactions to the large stabilization energy of alternative tautomer OQNH having increased basicity at the nitrogen atom and increased acidity at the oxygen atom (Figure 2). The attractive interaction of two opposite charges in a heterocyclic ring is also supposed to hinder the reverse reactions. For the cases of naphthols and their derivatives, reverse protonation following photodissociation is known to occur in acidic media.[7,20,21,23] Figure 5 shows the hypsochromic solvatochromism of tautomeric fluorescence, which shifts to the blue with the increase of the solvent dielectric constant. The tautomeric species of $^-OQNH^+$, the lowest excited

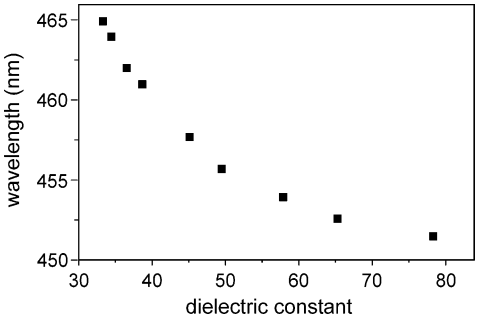

Figure 5. Fluorescence maximum wavelengths of OQNH with the dielectric constants of methanol/water−mixed solvents. Samples were excited at 320 nm, and dielectric constants were calculated from ref 48.

configuration of which is (π, π^*),[26] is expected to show a bathochromic shift. This indicates that the dipole moment of the emitting tautomer in the excited state is much smaller than that of $^-$OQNH$^+$ in the ground state. Considering the production of quinonoid species immediately following the formation of the prototropic zwitterionic species in the excited state of 6-hydroxyquinoline,[17,34] we then suggest that OQNH, drawn in Figure 2, results from tautomerization following intramolecular electronic charge transfer. The stabilization of the ground state by H bonds[46] and solvent-separated ion-pair interactions[47] could also contribute to the hypsochromic solvatochromism. Stabilization by the latter interactions is negligible for $^-$OQNH$^+$ in water because both positive and negative charges exist in a ring. However, weaker H bonds at the excited state are expected to induce negative solvatochromism as well, as found in naphtholate anions.[46] It is noteworthy that the magnitude of the hypsochromic shift for the tautomer of 3HQ is smaller than that for the tautomer of 6-hydroxyquinoline.[34] This reflects the fact that intramolecular electronic charge transfer takes place to a smaller extent in 3HQ, having two prototropic groups in close proximity to each other, and that electron rearrangement is indeed the major reason for the hypsochromic shift.

Arrhenius Plots of Proton-Transfer Rates. We have also measured the temperature dependence of 3HQ fluorescence kinetics with pH variation at various emission wavelengths to understand the complicated mechanism of excited-state tautomerization explicitly (Figure 6 and Table 2). The enol deprotonation of HOQNH$^+$ monitored at pH 2 and 400 nm gives an activation energy of 7.0 kJ mol^{-1}, whereas that of HOQN monitored at pH 6 and 350 nm shows an activation energy of 6.0 kJ mol^{-1}. It is interesting that the enol deprotonation of HOQNH$^+$ is 10 times faster than that of HOQN, whereas the activation energy of the deprotonation is even higher by 1.0 kJ mol^{-1}. The faster rate of HOQNH$^+$ can be accounted for by its net positive charge. The attractive interaction of a true positive charge with the negative partial charge of the oxygen atom makes the positive partial charge of the dissociating hydrogen relatively isolated and large enough to interact easily with a nearby water cluster. Water clusters are reported to be necessary for the proton transfer of acids and bases in water.[20−24,30] The preexponential factor of HOQNH$^+$ deprotonation, 15 times higher than that of HOQN deprotonation, also supports the fact that the formation rate of a water cluster near the enol group is enhanced by the positive charge of HOQNH$^+$. The activation energy of HOQNH$^+$ deprotonation, larger than that of HOQN deprotonation despite the faster rate, suggests that HOQNH$^+$ is energetically closer to the tautomeric species of $^-$OQNH$^+$ than to the normal species of HOQN. This also supports the previously discussed idea that the fluorescing tautomer of

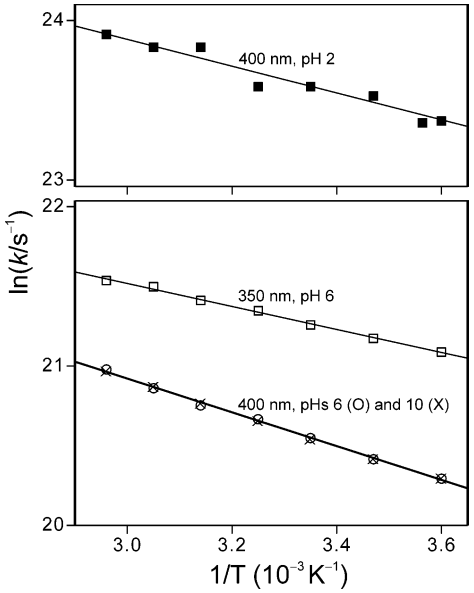

Figure 6. Arrhenius plots for the fluorescence decay rates at designated wavelengths of aqueous 3HQ solutions having indicated pH values.

TABLE 2: Kinetic Isotope Effects (KIEs), Activation Energies (E_a), and Preexponential Factors (A) of Proton Transfer for 3HQ Prototropic Species

λ_{em} (nm)	pH	species	process	KIE[a]	E_a (kJ mol^{-1})	A (s^{-1})
400	2	HOQNH$^+$	OH deprotonation	3.0	7.0	3×10^{11}
400	10	$^-$OQN	N protonation	1.8	8.8	3×10^{10}
350	6	HOQN	OH deprotonation	2.2	6.0	2×10^{10}
400	6	$^-$OQN	N protonation	1.8	8.8	3×10^{10}

[a] Measured at 25 °C.

OQNH is produced by electronic rearrangement following the formation of $^-$OQNH$^+$ by prototropic tautomerization. However, the activation energy for the imine protonation of $^-$OQN is 8.8 kJ mol^{-1} at pHs 6 and 10. These values are considered to be large because $^-$OQN is energetically even closer to $^-$OQNH$^+$ than is HOQNH$^+$.

Reaction Pathways Dependent on pH. The observed formation of OQNH emission is faster than the observed decay of intermediate emission in weakly acidic solutions (Figure 7a). The rise time of OQNH fluorescence should be the same as the emission decay time of the precursor intermediate; otherwise, there is a fast additional channel. Considering Figure 7a and the time constants of Table 1, we propose that tautomerization by excited-state proton transfers at 25 °C consists of several pathways as shown in eqs 1−4 and that the relative contribution of each pathway is dependent on pH.

$$\text{HOQN} \xrightarrow[600\ \text{ps}]{H_2O\ H_3O^+} {}^-\text{OQN} \xrightarrow[\text{fast}]{H_3O^+\ H_2O} {}^-\text{OQNH}^+ \left(\xrightarrow[\text{fast}]{} \text{OQNH}\right) \quad (1)$$

$$\text{HOQN} \xrightarrow[600\ \text{ps}]{H_2O\ H_3O^+} {}^-\text{OQN} \xrightarrow[1200\ \text{ps}]{H_2O\ OH^-} {}^-\text{OQNH}^+ \left(\xrightarrow[\text{fast}]{} \text{OQNH}\right) \quad (2)$$

$$\text{HOQNH}^+ \xrightarrow[60\ \text{ps}]{H_2O\ H_3O^+} {}^-\text{OQNH}^+ \left(\xrightarrow[\text{fast}]{} \text{OQNH}\right) \quad (3a)$$

$$\text{HOQN} \xrightarrow[\text{fast}]{H_3O^+\ H_2O} \text{HOQNH}^+ \xrightarrow[60\ \text{ps}]{H_2O\ H_3O^+} {}^-\text{OQNH}^+ \left(\xrightarrow[\text{fast}]{} \text{OQNH}\right) \quad (3b)$$

$$ {}^-\text{OQN} \xrightarrow[1200\ \text{ps}]{H_2O\ OH^-} {}^-\text{OQNH}^+ \left(\xrightarrow[\text{fast}]{} \text{OQNH}\right) \quad (4a)$$

$$\text{HOQN} \xrightarrow[\text{fast}]{OH^-\ H_2O} {}^-\text{OQN} \xrightarrow[1200\ \text{ps}]{H_2O\ OH^-} {}^-\text{OQNH}^+ \left(\xrightarrow[\text{fast}]{} \text{OQNH}\right) \quad (4b)$$

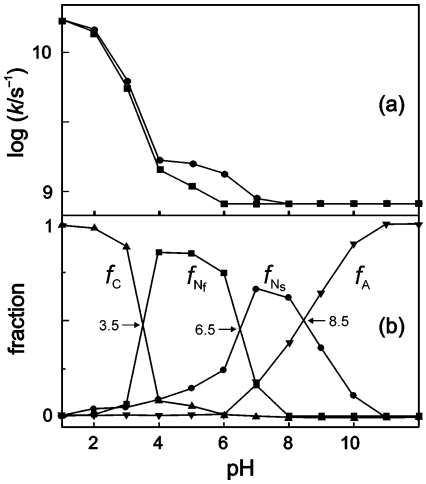

Figure 7. (a) Logarithmic fluorescence rate constants of aqueous 3HQ solutions with pH changes. The rise constants of tautomer fluorescence at 500 nm (●) are larger under weakly acidic conditions than the decay constants of intermediate fluorescence at 400 nm (■). (b) Fractional pathway contributions with pH changes for the excited-state tautomerization of aqueous 3HQ.

Because all of the rate constants are invariable regardless of apparent kinetic variation with pH, we can calculate the individual fractional contributions of f_{Nf}, f_{Ns}, f_C, and f_A for eqs 1−4, respectively. The following relations can be assumed at every measured pH:

$$1 = f_{Nf} + f_{Ns} + f_C + f_A \tag{5}$$

$$\tau_I/\text{ps} = \frac{1200f_{Ns} + 60f_C + 1200f_A}{f_{Ns} + f_C + f_A} \tag{6}$$

$$\tau_T/\text{ps} = 600f_{Nf} + 1200f_{Ns} + 60f_C + 1200f_A \tag{7}$$

$$\frac{\tau_N}{\tau_I} \times \frac{A_N}{A_I} = \frac{600f_{Nf} + 600f_{Ns}}{1200f_{Nf} + 60f_C + 1200f_A} \times \frac{(\nu_{350})^3}{(\nu_{400})^3} \times \frac{S_{350}}{S_{400}} \tag{8}$$

Although eq 5 is trivial, eqs 6 and 7 show that the observed intermediate decay time (τ_I) and the observed OQNH rise time (τ_T) are the weighted averages of the respectively involved times. The left and the right parts of eq 8 indicate the observed and the calculated intensity ratios, respectively, of HOQN emission to intermediate emission. τ_N is the observed emission lifetime of HOQN, whereas A_N and A_I are the initial emission intensities of HOQN and the intermediate species, respectively. S and ν are the detector sensitivity and the emission frequency, respectively, at each wavelength shown in nanometers. It is assumed in eq 8 that the Einstein coefficients of spontaneous emission for HOQN and intermediate species are the same except for the cubic dependence on the emission frequency because fluorescence is emitted from the same aromatic chromophore for all of the prototropic species involved. Each fraction should of course be no smaller than 0 and no larger than 1.

The detailed individual catalytic roles of H_2O, H_3O^+, and OH^- for the excited-state tautomerization of 3HQ in water are presented as functions of pH in Figure 7b. Because the HOQN species is excited more efficiently than the other prototropic species, tautomerization is catalyzed predominantly by H_2O following the pathways of eqs 1 and 2 in the broad pH region of 3.5−8.5. Because 3HQ exists mainly as $HOQNH^+$ below pH 3.5 and $^-$OQN above pH 8.5 at the moment of excitation, the tautomerization occurs following eq 3 below pH 3.5 and eq 4 above pH 8.5. It is noteworthy that tautomerization is catalyzed faster by H_2O (eq 1) than by OH^- (eq 4b). In the pathway of eq 1, the release of a proton from the enol group initiates the formation of a hydrated proton cluster, which directly participates via migration in the protonation of the imino group over a distance within a very short period of time. This can be explained by the fact that $^-$OQN formed in eq 1 does not have a hydrated proton cluster from the bulk solvent within the reaction cross section of the imino group. If there is such a proton cluster near the nitrogen atom of the imino group, either pathway in eq 3 will prevail over the process of eq 1.

Simulation studies have shown that proton diffusion occurs through the migration of a structural defect via continual interconversion between covalent and hydrogen bonds rather than through the hydrodynamic Stokes diffusion of a rigid complex.[12] A proton migrates as $H_9O_4^+$ is converted to $H_5O_2^+$ by a structural defect displaced over a distance of 2.5 Å. The proton in the complex of $H_9O_4^+$ or $H_5O_2^+$ is reported to be highly delocalized via hydrogen bonds.[11,12] Solvent fluctuations modulate the barriers of proton transfer and determine the migration path that occurs.[13] The hydrated proton cluster initially generated from the enol deprotonation of HOQN migrates within a few picoseconds to another cluster near the nitrogen atom of concurrently produced $^-$OQN via a few structural defects to convert the anion into $^-OQNH^+$ rapidly. This explains why the observed formation of OQNH emission is faster than the observed decay of intermediate emission in the pH range of 4−6 (Figure 7a). In addition, f_{Nf} under weakly acidic conditions is significantly larger in 3HQ than in 6-hydroxyquinoline.[17] This implies that the participation of proton migration in the tautomerization of molecular species 3HQ is much greater than that in the tautomerization of 6-hydroxyquinoline because two prototropic groups of enol and imine are located nearby. Thus, our results provide experimental evidence of the idea that the extremely fast diffusion of protons in water occurs by continuously forming and breaking hydrogen bonds involved in protonated water clusters.

In summary, we have measured fluorescence kinetics as functions of wavelength, pH, hydrogen isotope, and temperature to understand proton transfers involved in the tautomerization of excited 3HQ in water. The tautomerization of excited 3HQ in water occurs on the time scale of 1200 ps in a stepwise manner via forming the anionic intermediate of $^-$OQN in 600 ps. The pathway is energetically selected, owing to fact that the energy of $^-$OQN is lower than that of $HOQNH^+$. The anionic intermediate species of $^-$OQN transforms quickly into $^-OQNH^+$ in the pH region of 4−6 thanks to the rapidly migrating proton concurrently formed with the intermediate. The proton migration is suggested to proceed by the continuous formation and breakage of hydrogen bonds involved in the hydrated proton cluster. However, the tautomer of $^-OQNH^+$ is found to undergo electron rearrangement immediately to form the more stable tautomer of OQNH.

Acknowledgment. The Strategic National R&D Program is appreciated for the grant (M1-0214-00-0108). We also acknowledge the Center for Molecular Catalysis and the Brain Korea 21 Program. O.-H.K. thanks the Young-Do Foundation for a generous scholarship.

References and Notes

(1) Stubbe, J.; Nocera, D. G.; Yee, C. S.; Chang, M. C. Y. *Chem. Rev.* **2003**, *103*, 2167.
(2) Ceulemans, J. *Acc. Chem. Res.* **2002**, *35*, 523.
(3) Kirby, A. J. *Acc. Chem. Res.* **1997**, *30*, 290.

(4) Douhal, A.; Lahmani, F.; Zewail, A. H. *Chem. Phys.* **1996**, *207*, 477.
(5) Catalán, J.; Pérez, P.; del Valle, J. C.; de Paz, J. L. G.; Kasha, M. *Proc. Natl. Acad. Sci. U.S.A.* **2002**, *99*, 5793.
(6) Kim, S.; Kim, T.-G.; Ah, C. S.; Kim, K.; Jang, D.-J. *J. Phys. Chem. B* **2004**, *108*, 880.
(7) Tolbert, L. M.; Solntsev, K. M. *Acc. Chem. Res.* **2002**, *35*, 19.
(8) Solntsev, K. M.; Tolbert, L. M.; Cohen, B.; Huppert, D.; Hayashi, Y.; Feldman, Y. *J. Am. Chem. Soc.* **2002**, *124*, 9046.
(9) Solntsev, K. M.; Huppert, D.; Agmon, N. *Phys. Rev. Lett.* **2001**, *86*, 3427. Solntsev, K. M.; Huppert, D.; Agmon, N. *J. Phys. Chem. A* **2001**, *105*, 5868. Solntsev, K. M.; Agmon, N. *Chem. Phys. Lett.* **2000**, *320*, 262.
(10) Cohen. B.; Huppert, D.; Agmon, N. *J. Phys. Chem. A* **2001**, *105*, 7165.
(11) Marx, D.; Tuckerman, M. E.; Hutter, J.; Parrinello, M. *Nature* **1999**, *397*, 601.
(12) Tuckerman, M. E.; Marx, D.; Klein, M. L.; Parrinello, M. *Science* **1997**, *275*, 817.
(13) Kornyshev, A. A.; Kuznetsov, A. M.; Spohr, E.; Ulstrup, J. *J. Phys. Chem. B* **2003**, *107*, 3351.
(14) Walrafen, G. E.; Chu, Y. C.; Carlon, H. R. *J. Phys. Chem. A* **2002**, *106*, 933.
(15) Yu, W.-S.; Cheng, C.-C.; Cheng, Y.-M.; Wu, P.-C.; Song, Y.-H.; Chi, Y.; Chou, P.-T. *J. Am. Chem. Soc.* **2003**, *125*, 10800.
(16) Kwon, O.-H.; Doo, H.; Lee, Y.-S.; Jang, D.-J. *ChemPhysChem* **2003**, *4*, 1079.
(17) Kim, T. G.; Kim, Y.; Jang, D.-J. *J. Phys. Chem. A* **2001**, *105*, 4328.
(18) Agmon, N.; Rettig, W.; Groth, C. *J. Am. Chem. Soc.* **2002**, *124*, 1089.
(19) Solntsev, K. M.; Huppert, D.; Tolbert, L. M.; Agmon, N. *J. Am. Chem. Soc.* **1998**, *120*, 7981.
(20) Tolbert, L. M.; Haubrich, J. E. *J. Am. Chem. Soc.* **1994**, *116*, 10593.
(21) Webb, S. P.; Philips, L. A.; Yeh, S. W.; Tolbert, L. M.; Clark, J. H. *J. Phys. Chem.* **1986**, *90*, 5154.
(22) Fillingim, T. G.; Luo, N.; Lee, J.; Robinson, G. W. *J. Phys. Chem.* **1990**, *94*, 6368.
(23) Lee, J.; Robinson, G. W.; Webb, S. P.; Philips, L. A.; Clark, J. H. *J. Am. Chem. Soc.* **1986**, *108*, 6538.
(24) Robinson, G. W.; Thistlethwaite, P. J.; Lee, J. *J. Phys. Chem.* **1986**, *90*, 4224.
(25) Kohtani, S.; Tagami, A.; Nakagaki, R. *Chem. Phys. Lett.* **2000**, *316*, 88.
(26) Fang, W.-H. *J. Am. Chem. Soc.* **1998**, *120*, 7568.
(27) Tanner, C.; Manca, C.; Leutwyler, S. *Science* **2003**, *302*, 1736.
(28) Bardez, E. *Isr. J. Chem.* **1999**, *39*, 319.
(29) Coussan, S.; Bach, A.; Leutwyler, S. *J. Phys. Chem. A* **2000**, *104*, 9864.
(30) Bardez, E.; Fedorov, A.; Berberan-Santos, M. N.; Martinho, J. M. G. *J. Phys. Chem. A* **1999**, *103*, 4131.
(31) Bach, A.; Hewel, J.; Leutwyler, S. *J. Phys. Chem. A* **1998**, *102*, 10476.
(32) Lee, S.-I.; Jang, D.-J. *J. Phys. Chem.* **1995**, *99*, 7537.
(33) Kim, T.-G.; Lee, S.-I.; Jang, D.-J.; Kim, Y. *J. Phys. Chem.* **1995**, *99*, 12698.
(34) Bardez, E.; Chatelain, A.; Larrey, B.; Valeur, B. *J. Phys. Chem.* **1994**, *98*, 2357.
(35) Yao, S. H.; Lee, J.; Robinson, G. W. *J. Am. Chem. Soc.* **1990**, *112*, 5698.
(36) Tokay, N.; Ögretir, C. *J. Mol. Struct.: THEOCHEM* **2002**, *594*, 185.
(37) Bardez, E.; Devol, I.; Larrey, B.; Valeur, B. *J. Phys. Chem. B* **1997**, *101*, 7786.
(38) Mason, S. F.; Philp, J.; Smith, B. E. *J. Chem. Soc. A* **1968**, 3051.
(39) Poizat, O.; Bardez, E.; Buntinx, G.; Alain, V. *J. Phys. Chem. A* **2004**, *108*, 1873.
(40) Albert, A.; Phillips, J. N. *J. Chem. Soc.* **1956**, 1294. Abramovitch, R. A. *J. Chem. Soc.* **1954**, 3839.
(41) Bates, R. G. *Determination of pH*; John Wiley & Sons: New York, 1973; Chapter 11.
(42) Pines, E.; Huppert, D.; Gutman, M.; Nachliel, N.; Fishman, M. *J. Phys. Chem.* **1986**, *90*, 6366.
(43) Mente, S.; Maroncelli, M. *J. Phys. Chem. A* **1998**, *102*, 3860.
(44) Kyrychenko, A.; Stepanenko, Y.; Waluk, J. *J. Phys. Chem. A* **2000**, *104*, 9542.
(45) Agmon, N. *Chem. Phys. Lett.* **1995**, *244*, 456.
(46) Solntsev, K. M.; Huppert, D.; Agmon, N. *J. Phys. Chem. A* **1998**, *102*, 9599.
(47) Soumillion, J. Ph.; Vandereecken, P.; Van Der Auweraer, M.; De Schryver, F. C.; Schanck, A. *J. Am. Chem. Soc.* **1989**, *111*, 2217.
(48) Solntsev, K. M.; Huppert, D.; Agmon, N.; Tolbert, L. M. *J. Phys. Chem. A* **2000**, *104*, 4658.